

Spotlight inversion by orthogonal projections

D Calvetti¹ N Hyvönen² V Kolehmainen³ E Somersalo¹

¹ Case Western Reserve University, Cleveland, OH, USA

² Aalto University, Espoo, Finland

³ University of Eastern Finland, Kuopio, Finland

Abstract

In inverse problems, the goal is to estimate unknown parameters from indirect noisy observations. It is not uncommon that the forward model assigning the observed variables to given values of the unknowns depend on variables that are not of primary interest, often referred to as nuisance parameters. In this article, we consider linear inverse problems, and propose a novel technique, based on linear algebra and orthogonal projections, to eliminate, or at least mitigate, the contribution of the nuisance parameters on the data. The approach is referred to as spotlight inversion, as it allows to focus on the part of primary interest of the unknown parameter, leaving the uninteresting part in the shadow. The viability of the approach is demonstrated by a computed example of local fanbeam X-ray tomography: the spotlight is on the region of interest that is part of the full target.

1 Introduction

In numerous applications in science and engineering it becomes necessary to solve an inverse problem that can be formulated as follows: Given a linear observation model

$$b = Ax + \varepsilon,$$

where $A \in \mathbb{R}^{m \times n}$ is a known matrix, b is a measured quantity, and ε is random additive noise, the problem is to estimate *selected components* of the vector $x \in \mathbb{R}^n$. Without loss of generality, we can permute the entries of x so that the quantity of interest consists of its first n_1 components, $n_1 < n$. By partitioning the matrix A accordingly, we can reformulate the inverse problem as

$$b = A_1 x_1 + A_2 x_2 + \varepsilon, \tag{1}$$

where $A_j \in \mathbb{R}^{m \times n_j}$, $j = 1, 2$ are known matrices, $n_1 + n_2 = n$.

Inverse problems of the form (1) arise in different contexts, including the following important applications.

Local tomography: In local X-ray tomography, the measured X-ray attenuation data depends on the absorption properties of the body extending over the entire field of view of the imaging system, although

only a portion of the domain, often referred to as region of interest (ROI) corresponding to x_1 , may be of interest. Local tomography commonly arises in X-ray tomography applications, either because of limited detector size, e.g., in dental Cone Beam Computed Tomography (CBCT) or because of the need to reduce the X-ray dose outside of the ROI, e.g., in cardiac imaging.

Radar imaging: In radar imaging, the signal comprises the signal of interest coming from the main lobe of the radar, corresponding to x_1 , and the radar clutter from the radar sidelobes that pick up the echo of trees, ground etc., represented by x_2 .

Image deblurring: A blurred image typically accounts for the contribution from both the field of view and leak data from the outside region. Inappropriate modeling or ignoring of the latter may cause boundary artifacts that are often compensated for by means of artificial boundary conditions.

MEG/EEG based brain imaging: The search for the onset foci of epileptic seizures often can be restricted to a portion of the brain; Likewise, localization of active brain regions constituting a task-related, or task-negative connected network may be limited to selected brain regions.

Functional MRI imaging: Identification of a stimulus-related cerebral activity of interest typically may be circumscribed to a known part of the brain, and the dynamics of the rest of the brain and other tissues is of less or no interest.

In statistics, the portion of the unknown x_2 in (1) not of interest is referred to as *nuisance parameters* while the radar community refer to the contribution A_2x_2 to the noiseless signal Ax as *clutter*. In this paper we adopt the terminology from both these two communities.

In the literature, the problem of separating the portion of interest from the clutter has been addressed in different ways. The tools for nuisance parameter elimination in classical statistics include considerations of sufficient and ancillary statistics and likelihood ratios [2, 11]. Bayesian statistics addresses the problem typically through integrated likelihood methods [3] or marginalization over the nuisance parameter, often requiring MCMC sampling [6]. An example of optimization-based methods of estimating nuisance parameters in inverse problems can be found in [1]. In a naïve approach, the nuisance parameter x_2 can be fixed to a plausible or representative value, or ignored by setting $x_2 = 0$, typically introducing a bias that in the Bayesian setting can be compensated by appropriate error modeling using the prior distribution of x_2 [9].

In this article, we put the spotlight of the inversion process on the portion x_1 of the unknown using a linear algebra-based approach exploiting suitable orthogonal projections. We begin by outlining the idea when the dimensionality of the nuisance parameter does not exceed that of the data, $m > n_2$, then discuss how to extend it to more general settings.

Let

$$P : \mathbb{R}^m \rightarrow \mathcal{R}(A_2), \quad P^\perp : \mathbb{R}^m \rightarrow \mathcal{R}(A_2)^\perp = \mathcal{N}(A_2^\top),$$

denote the pair of orthogonal projectors onto the range $\mathcal{R}(A_2) \subset \mathbb{R}^m$ of the matrix A_2 and onto the null space $\mathcal{N}(A_2^\top)$ of the matrix A_2^\top , respectively. The assumption $m > n_2$ guarantees that the subspace $\mathcal{N}(A_2^\top)$ is non-trivial. Applying P^\perp to both sides of (1) and observing that $P^\perp A_2 x_2 = 0$ yields

$$b' = A'_1 x_1 + \varepsilon', \tag{2}$$

where $b' = P^\perp b$, $A'_1 = P^\perp A_1$, $\varepsilon' = P^\perp \varepsilon$. The projected problem, which does not contain the nuisance parameters can be solved by any standard regularization technique, or, alternatively, it can be analyzed in

the framework of Bayesian inverse problems: see Section 2.

The assumption that the clutter is restricted to a proper subspace of \mathbb{R}^m , is automatically satisfied in the case of overdetermined problems where $m > n > n_2$. The relation of the projection-based approach with the classical likelihood splitting techniques and marginalization methods in statistics will be discussed in the next section. It is possible to generalize the approach to the general case via a partial projection technique, as explained section 3. Extensions to non-linear inverse problems are briefly discussed in section 5.

2 Spotlight projections in the Bayesian framework

In this section, we provide a Bayesian interpretation of spotlight projection method, under the assumption of Gaussian prior and Gaussian likelihood. We begin by outlining standard techniques to deal with nuisance parameters on marginalization and modeling the clutter as part of the noise. For a general reference on the Bayesian solution of linear inverse problems, see, e.g., [5].

2.1 Marginalization and error modeling

In the Bayesian extension of the inverse problem (1), let X denote a \mathbb{R}^n -valued Gaussian random variable with prior probability density $X \sim \mathcal{N}(0, C)$, where $n = n_1 + n_2$, and $C \in \mathbb{R}^{n \times n}$ is a symmetric positive definite covariance matrix. We partition X and the forward model

$$X = \begin{bmatrix} X_1 \\ X_2 \end{bmatrix}, \quad X_j \in \mathbb{R}^{n_j}, \quad A = \begin{bmatrix} A_1 & A_2 \end{bmatrix} \in \mathbb{R}^{m \times n},$$

and write the stochastic extension of the model as

$$B = AX + E = A_1X_1 + A_2X_2 + E,$$

where E is an additive Gaussian noise vector independent of X . Without loss of generality, we may assume that the noise is whitened, i.e., $E \sim \mathcal{N}(0, I)$. Furthermore, we partition the prior covariance matrix as

$$C = \begin{bmatrix} C_{11} & C_{12} \\ C_{21} & C_{22} \end{bmatrix}, \quad C_{jk} \in \mathbb{R}^{n_j \times n_k}.$$

The estimation of the variable X_1 based on the observation B , may be done in two different ways:

1. *Lumping and conditioning*: Write the forward model as

$$B = A_1X_1 + (A_2X_2 + E) = A_1X_1 + \hat{E},$$

interpreting the clutter term as part of the observation noise $\hat{E} = A_2X_2 + E$, and then calculate directly the posterior density $\pi_{X_1|B}(x_1 | b)$ by conditioning.

2. *Marginalization:* Calculate the posterior probability density of (X_1, X_2)

$$\pi_{X|B}(x | b) = \pi_{X_1, X_2|B}(x_1, x_2 | b),$$

and then marginalize it with respect to X_2 ,

$$\pi_{X_1|B}(x_1 | b) = \int \pi_{X_1, X_2|B}(x_1, x_2 | b) dx_2.$$

While it is intuitively clear that these two approaches should lead to the same posterior density, for completeness we state this as a theorem and give a short proof of it.

Theorem 2.1 *Under the above hypotheses, the derivations of the posterior density $\pi_{X_1|b}(x_1 | b)$ via conditioning and marginalization are equivalent. Moreover, the posterior is a Gaussian density,*

$$X_1 | B \sim \mathcal{N}(\mu_1, D_1),$$

with mean and covariance

$$\mu_1 = (C_{11}A_1^T + C_{12}A_2^T)(ACA^T + I)^{-1}b, \quad D_1 = C_{11} - (C_{11}A_1^T + C_{12}A_2^T)(ACA^T + I)^{-1}(A_1C_{11} + A_2C_{21}).$$

Proof. Conditioning approach. Combine X_1 and B into the Gaussian random variable

$$Z = \begin{bmatrix} X_1 \\ B \end{bmatrix}.$$

From the observations that

$$\mathbb{E}(X_1X_1^T) = C_{11}, \quad \mathbb{E}(X_1B^T) = C_{11}A_1^T + C_{12}A_2^T = \mathbb{E}(BX_1^T)^T,$$

and

$$\mathbb{E}(BB^T) = \mathbb{E}((AX + E)(AX + E)^T) = ACA^T + I,$$

it follows that

$$\mathbb{E}(ZZ^T) = D = \begin{bmatrix} D_{11} & D_{12} \\ D_{21} & D_{22} \end{bmatrix} = \begin{bmatrix} C_{11} & C_{11}A_1^T + C_{12}A_2^T \\ A_1C_{11} + A_2C_{21} & ACA^T + I \end{bmatrix}.$$

Thus, the mean and the covariance matrix of X_1 conditional on $B = b$ can be expressed in terms of the Schur complement of D_{22} as

$$\begin{aligned} \mathbb{E}(X_1 | B = b) &= (C_{11}A_1^T + C_{12}A_2^T)(ACA^T + I)^{-1}b, \\ \text{cov}(X_1 | B = b) &= C_{11} - (C_{11}A_1^T + C_{12}A_2^T)(ACA^T + I)^{-1}(A_1C_{11} + A_2C_{21}), \end{aligned}$$

which agree with the expressions given in the theorem.

Marginalization approach. The joint posterior density of the random variable $X = [X_1; X_2]^T$ given $B = b$ is

$$\pi_{X_1, X_2|B}(x_1, x_2 | b) = \mathcal{N}(x | \mu, D), \quad \mu = CA^T(ACA^T + I)^{-1}b, \quad D = C - CA^T(ACA^T + I)^{-1}AC.$$

It can be shown, after completing the square and computing Schur complements, that the marginal density of X_1 is

$$\pi_{X_1|B}(x_1 | b) = \mathcal{N}(x_1 | \mu_1, D_{11}),$$

where μ_1 and D_{11} refer to block partitionings of the posterior mean and covariance,

$$\mu = \begin{bmatrix} \mu_1 \\ \mu_2 \end{bmatrix}, \quad D = \begin{bmatrix} D_{11} & D_{12} \\ D_{21} & D_{22} \end{bmatrix}.$$

Recalling that

$$CA^T = \begin{bmatrix} C_{11} & C_{12} \\ C_{21} & C_{22} \end{bmatrix} \begin{bmatrix} A_1^T \\ A_2^T \end{bmatrix} = \begin{bmatrix} C_{11}A_1^T + C_{12}A_2^T \\ C_{21}A_1^T + C_{22}A_2^T \end{bmatrix},$$

we obtain

$$\mu_1 = (C_{11}A_1^T + C_{12}A_2^T)(ACA^T + I)^{-1}b,$$

and

$$D_{11} = C_{11} - (C_{11}A_1^T + C_{12}A_2^T)(ACA^T + I)^{-1}(A_1C_{11} + A_2C_{21}),$$

thus we find that the density is the same as what we found in the previous part. \square

2.2 Projection versus marginalization

The density of X_1 obtained through marginalization differs from the posterior density of the projected problem (2) because the former depends on both Pb and $P^\perp b$. To shed some light on how the projection method relates to the marginalization approach, we write

$$\begin{aligned} \|b - A_1x_1 - A_2x_2\|^2 &= \|P^\perp(b - A_1x_1 - A_2x_2) + P(b - A_1x_1 - A_2x_2)\|^2 \\ &= \|b' - A'_1x_1\|^2 + \|b'' - A_2x_2 - A''_1x_1\|^2, \end{aligned}$$

where

$$b'' = Pb, \quad A''_1 = PA_1.$$

and substitute this decomposition into the whitened likelihood model $\pi_{B|X}(b | x)$ to obtain

$$\begin{aligned} \pi_{B|X}(b | x) &\propto \exp\left(-\frac{1}{2}\|b' - A'_1x_1\|^2\right) \exp\left(-\frac{1}{2}\|b'' - A_2x_2 - A''_1x_1\|^2\right) \\ &\propto \pi_{B'|X_1}(b' | x_1) \pi_{B''|X_1, X_2}(b'' | x_1, x_2). \end{aligned} \tag{3}$$

If, in addition, X_1 and X_2 are Gaussian and mutually independent, the joint prior factors as

$$\pi_X(x) = \pi_{X_1, X_2}(x_1, x_2) = \pi_{X_1}(x_1) \pi_{X_2}(x_2),$$

and the posterior distribution can be written as

$$\begin{aligned} \pi_{X_1, X_2|B}(x_1, x_2 | b) &\propto \underbrace{\pi_{B'|X_1}(b' | x_1) \pi_{B''|X_1, X_2}(b'' | x_1, x_2)}_{(a)} \underbrace{\pi_{X_1}(x_1) \pi_{X_2}(x_2)}_{(b)} \\ &= \underbrace{\pi_{X_1}(x_1) \pi_{B'|X_1}(b' | x_1)}_{(a)} \underbrace{\pi_{X_2}(x_2) \pi_{B''|X_1, X_2}(b'' | x_1, x_2)}_{(b)}, \end{aligned}$$

where (a) coincides with the posterior of the projected model. In general, since (b) depends on x_1 , it cannot be ignored. The fact that marginalization with respect to x_2 will give a contribution to the posterior density of X_1 , complicates the Bayesian interpretation of the projected problem in the general case.

The theorem below states that the posterior of the projected problem converges to the marginal density as the prior for X_2 becomes asymptotically uninformative. More specifically, assume that the prior for X_2 is of the form

$$\pi_{X_2}(x_2) = \pi_{X_2}^\alpha(x_2) \sim \mathcal{N}(0, \alpha^{-2}\mathbf{G}),$$

where \mathbf{G} is a symmetric positive definite matrix, and $\alpha > 0$ is a scaling parameter. Without loss of generality, possibly via a whitening transformation, we assume that $\mathbf{G} = \mathbf{I}$. As $\alpha \rightarrow 0$, the prior distribution of X_2 becomes increasingly wide, and the prior becomes asymptotically uninformative. In the following theorem, we denote by $\pi_{X_1, X_2|B}^\alpha$ the conditional joint density when the prior for X_2 is chosen as a function of α in this manner.

Theorem 2.2 *Assume that $\mathbf{A}_2 \in \mathbb{R}^{m \times n_2}$ and $\text{rank}(\mathbf{A}_2) = n_2 < m$. As the prior for X_2 becomes uninformative, the marginal probability density of X_1 ,*

$$\pi_{X_1|B'}^\alpha(x_1 | b) = \int \pi_{X_1, X_2|B}^\alpha(x_1, x_2 | b) dx_2,$$

converges to the posterior density for the projected problem (2), i.e., for some constant $C > 0$,

$$\lim_{\alpha \rightarrow 0} \alpha^{-n_2} \pi_{X_1|B'}^\alpha(x_1 | b') = C \pi_{X_1}(x_1) \pi_{B'|X_1}(b' | x_1).$$

Proof: We want to prove that in the limit $\alpha \rightarrow 0$, the integral

$$I_\alpha = \int \pi_{X_2}^\alpha(x_2) \pi_{B''|X_1, X_2}(b'' | x_1, x_2) dx_2,$$

is independent of x_1 . To that end, we observe that

$$\begin{aligned} \|b'' - \mathbf{A}_2 x_2 - \mathbf{A}_1'' x_1\|^2 + \alpha^2 \|x_2\|^2 &= x_2^\top (\mathbf{A}_2^\top \mathbf{A}_2 + \alpha^2 \mathbf{I}) x_2 - 2x_2^\top \mathbf{A}_2^\top (b'' - \mathbf{A}_1'' x_1) + \|b'' - \mathbf{A}_1'' x_1\|^2 \\ &= x_2^\top \mathbf{H}_\alpha x_2 - 2x_2^\top \mathbf{A}_2^\top y + \|y\|^2 \\ &= (x_2 - \mathbf{H}_\alpha^{-1} \mathbf{A}_2^\top y)^\top \mathbf{H}_\alpha (x_2 - \mathbf{H}_\alpha^{-1} \mathbf{A}_2^\top y) + \|y\|^2 - y^\top \mathbf{A}_2 \mathbf{H}_\alpha^{-1} \mathbf{A}_2^\top y, \end{aligned}$$

where

$$\mathbf{H}_\alpha = \mathbf{A}_2^\top \mathbf{A}_2 + \alpha^2 \mathbf{I} = \mathbf{H}_0 + \alpha^2 \mathbf{I}, \quad y = b'' - \mathbf{A}_1'' x_1.$$

Since \mathbf{A}_2 has full rank and \mathbf{H}_0 is invertible, we may use the resolvent identity

$$\mathbf{H}_\alpha^{-1} = \mathbf{H}_0^{-1} - \alpha^2 \mathbf{H}_0^{-1} \mathbf{H}_\alpha^{-1},$$

to write

$$y^\top \mathbf{A}_2 \mathbf{H}_\alpha^{-1} \mathbf{A}_2^\top y = y^\top \mathbf{A}_2 \mathbf{H}_0^{-1} \mathbf{A}_2^\top y - \alpha^2 y^\top \mathbf{A}_2 \mathbf{H}_0^{-1} \mathbf{H}_\alpha^{-1} \mathbf{A}_2^\top y.$$

Moreover, from $y \in \mathcal{R}(\mathbf{A}_2)$ and the definition of \mathbf{H}_0 we have $\mathbf{A}_2 \mathbf{H}_0^{-1} \mathbf{A}_2^\top y = y$, and $y^\top \mathbf{A}_2 \mathbf{H}_0^{-1} \mathbf{A}_2^\top y = y^\top y = \|y\|^2$, implying that

$$x_2^\top \mathbf{H}_\alpha x_2 - 2x_2^\top \mathbf{A}_2^\top y + \|y\|^2 = (x_2 - \mathbf{H}_\alpha^{-1} \mathbf{A}_2^\top y)^\top \mathbf{H}_\alpha (x_2 - \mathbf{H}_\alpha^{-1} \mathbf{A}_2^\top y) + \alpha^2 y^\top \mathbf{A}_2 \mathbf{H}_0^{-1} \mathbf{H}_\alpha^{-1} \mathbf{A}_2^\top y.$$

We can now evaluate the integral I_α ,

$$\begin{aligned} I_\alpha &= C' \alpha^{n_2} \int \exp \left(-\frac{1}{2} (\|b'' - A_2 x_2 - A_1'' x_1\|^2 + \alpha^2 \|x_2\|^2) \right) dx_2 \\ &= \frac{(2\pi)^{n_2/2} C' \alpha^{n_2}}{|\det(H_\alpha)|^{1/2}} \exp \left(-\frac{1}{2} \alpha^2 y^\top A_2 H_0^{-1} H_\alpha^{-1} A_2^\top y \right), \end{aligned}$$

where C' is a constant, and hence

$$\alpha^{-n_2} I_\alpha \rightarrow \frac{(2\pi)^{n_2/2} C'}{|\det(H_0)|^{1/2}} = C, \quad \text{as } \alpha \rightarrow 0.$$

This completes the proof. \square

For simplicity, the theorem assumed that the matrix $A_2 \in \mathbb{R}^{m \times n_2}$ has full rank. If $\text{rank}(A_2) = r < n_2$, then it follows from the lean SVD of A_2 ,

$$A_2 = \sum_{j=1}^r \sigma_j u_j (v_j)^\top = U_r D_r V_r,$$

that the clutter term is in an r -dimensional subspace of \mathbb{R}^m

$$A_2 x_2 = A_2 x'_2, \quad x'_2 = U_r U_r^\top x_2,$$

and the projectors are

$$P = U_r U_r^\top, \quad P^\perp = I - P.$$

Hence, we may replace n_2 by r . In particular, this calculation implies that the nuisance parameter in the model is effectively r -dimensional.

3 Partial projection, ill-determined rank and underdetermined problems

In the previous section, it was assumed that the dimensionality of the nuisance parameter does not exceed the dimension of the data space, and that the columns of the matrix A_2 are linearly independent, which may not always be satisfied in actual applications. If the rank of the matrix A_2 is ill-determined, i.e., some of its singular values are close to the computational precision, determining its effective rank is an ill-posed problem and the projectors may be very sensitive to roundoff errors. Furthermore, if the dimension of the nuisance parameter vector n_2 exceeds m , we may have $\mathcal{N}(A_2^\top) = \{0\}$ implying that $P^\perp = 0$ and the right hand side of the projected problem does not carry any information about x_1 .

In this section we illustrate how the projection method can be modified to address these cases. Let

$$A_2 = U D V^\top$$

be a complete SVD of A_2 . If $n_2 < m$ and A_2 is full rank, as we assumed in the previous section,

$$\lambda_1 \geq \dots \geq \lambda_{n_2} > 0, \quad \mathcal{R}(A_2) = \text{span}\{u_1, \dots, u_{n_2}\},$$

where $u_j \in \mathbb{R}^m$ is the j th column of U , and hence $P = U_{n_2} U_{n_2}^\top$, with $U_{n_2} = [u_1, \dots, u_{n_2}]$.

Replacing the exact projector P in the projected equation by its rank r approximation $P_r = \sum_{j=1}^r u_j u_j^\top$ for some $r \leq n_2$ yields

$$b'_r = P_r^\perp b = A'_{1,r} x_1 + P_r^\perp A_2 x_2 + \varepsilon'_r,$$

where

$$A'_{1,r} = P_r^\perp A_1, \quad \varepsilon'_r = P_r^\perp \varepsilon, \quad P_r^\perp = I - P_r = \sum_{j=r+1}^m u_j u_j^\top.$$

Observe that since

$$P_r^\perp A_2 = \sum_{j=r+1}^{n_2} \lambda_j u_j v_j^\top, \tag{4}$$

the projected clutter term vanishes if $r = n_2$. To estimate the expected size of the projected clutter we introduce the symmetric positive definite covariance matrix C_{22} of the random variable X_2 , the stochastic extension of the unknown vector x_2 . Hence,

$$\begin{aligned} \mathbb{E}(\|P_r^\perp A_2 X_2\|^2) &= \mathbb{E}(\text{Trace}(P_r^\perp A_2 X_2)(P_r^\perp A_2 X_2)^\top) \\ &= \text{Trace}(P_r^\perp A_2 \mathbb{E}(X_2 X_2^\top)(P_r^\perp A_2)^\top) \\ &= \text{Trace}(P_r^\perp A_2 C_{22} (P_r^\perp A_2)^\top) \\ &= \|P_r^\perp A_2 C_{22}^{1/2}\|_F^2 = \left\| \sum_{j=r+1}^{n_2} \lambda_j u_j (C_{22}^{1/2} v_j)^\top \right\|_F^2. \end{aligned}$$

Furthermore, it follows from the orthonormality of the vectors u_j that

$$\left\| \sum_{j=r+1}^{n_2} \lambda_j u_j (C_{22}^{1/2} v_j)^\top \right\|_F^2 = \sum_{j=r+1}^{n_2} \lambda_j^2 \|C_{22}^{1/2} v_j\|^2,$$

hence

$$\mathbb{E}(\|P_r^\perp A_2 X_2\|^2) \leq \|C_{22}\| \sum_{j=r+1}^{n_2} \lambda_j^2.$$

We proceed in a similar manner to estimate the expected size of the projected noise ε'_r . Letting E be the whitened stochastic extension of ε , $E \sim \mathcal{N}(0, I_m)$, we have that

$$\mathbb{E}(\|P_r^\perp E\|^2) = \text{Trace}(P_r^\perp I_m (P_r^\perp)^\top) = \text{Trace}\left(\sum_{j=r+1}^m u_j u_j^\top\right) = m - r.$$

Selecting the rank of the approximate projector as the smallest integer r for which the condition

$$\|C_{22}\| \sum_{j=r+1}^{n_2} \lambda_j^2 < m - r, \tag{5}$$

is satisfied ensures that the expected size of the residual clutter is smaller than the projected additive noise, thus the projected clutter term can be safely neglected in the projected problem. To have a computationally useful criterion for the truncation, we introduce the ratios

$$R_r = \frac{\|C_{22}\| \sum_{j=r+1}^{n_2} \lambda_j^2}{m - r}, \quad 0 \leq r < m. \quad (6)$$

Observe that for $r = 0$, the ratio

$$\text{cSNR} = \frac{\mathbb{E}(\|A_2 X_2\|^2)}{\mathbb{E}(\|E\|^2)}$$

represents the clutter signal-to-noise ratio, and we have the estimate

$$\text{cSNR} \leq \frac{\|C_{22}\| \sum_{j=1}^{n_2} \lambda_j^2}{m} = R_0.$$

When the upper bound R_0 on the right in the above inequality is less than one, we may conclude that the clutter is dominated by the additive noise, and no projection is necessary. If, on the other hand, $R_0 > 1$, the ratios R_r serve as a good indicator for selecting r . Observe that for $n_2 < m$, we have $\lim_{r \rightarrow n_2} R_r = 0$, and the truncation value r can be chosen as the smallest r for which

$$R_r < 1, \quad (7)$$

yielding an estimate for the the smallest r for which the inequality (5) is satisfied. For $n_2 \geq m$ there is no guarantee that the inequality $R_r < 1$ holds for any r , however, if it does, a feasible truncation value is the smallest r for which it holds. More generally, the value r that minimizes R_r gives the optimal clutter reduction.

3.1 Randomized spotlight projection

The SVD of the matrix A_2 may be unfeasible in practice if the matrix dimensions are large. This is typically the case when the spotlight inversion technique is applied to inverse problems with spatially distributed parameters in three dimensions, the voxel number easily arriving to millions and the only feasible way to operations by A_2 and A_2^T is to carry out computations without explicit formation of A_2 . In such cases, a natural remedy is to use randomized linear algebra and algorithms, see, e.g., [7, 12, 14] for results and further references. In particular, for a given integer k , one first forms a Gaussian random matrix

$$\Omega \in \mathbb{R}^{n_2 \times k}, \quad \Omega_{ij} \sim \mathcal{N}(0, 1).$$

Next, the matrix A_2 is applied to the columns of Ω , yielding the matrix $Z = A_2 \Omega$. It can be shown that with high probability, the range of the matrix Z gives a good approximation of the range of A_2 , and an orthonormal basis for the range of Z can be found with a relatively lightweight lean QR algorithm, or by calculating the lean SVD of Z , discarding singular values below the computational precision. We refer to the cited articles for more detailed discussion.

4 Application: Local tomography

As a demonstration of the viability of the spotlight inversion approach, and to test the truncation criteria for the approximate projections, we apply the method to a computed two-dimensional local tomography problem with real fanbeam data. As a general reference to local tomography, see, e.g., the monograph [13]. For a marginalization-based approach in the Bayesian inverse problems framework, we refer to [10].

The test case is based on an open access X-ray tomography data of a lotus plant root filled with different chemical elements [4]. The data set contains data for a 2D slice from fan beam scan of the target from 120 equally spaced angles over 360° rotation, and forward matrix for the experiment using a 128×128 discretization of an image domain that covers completely the scanned specimen.

Using this data, we formed a local tomography experiment by retrospective down-sampling of the data. We selected 40×40 pixel spotlight window (or region of interest, ROI) from the image domain and formed local tomography experiment by selecting the subset of X-rays that intersect the ROI, discarding all remaining data. This way, we ended having local tomography data $b \in \mathbb{R}^{14664}$ and forward model

$$b = Ax + \varepsilon = A_1x_1 + A_2x_2 + \varepsilon \quad (8)$$

with $x \in \mathbb{R}^{16384}$, $x_1 \in \mathbb{R}^{1600}$ and $x_2 \in \mathbb{R}^{14784}$. Observe that $n_2 > m$, so a full spotlight projection is not feasible.

The level of measurement noise in the experiment is not known. In the following, the noise E is modeled as Gaussian scaled white noise,

$$E \sim \mathcal{N}(0, \sigma^2 I) \quad (9)$$

with the noise standard deviation σ estimated from a empty space patch (i.e., rays observed outside the attenuating target) of the original data, leading to an estimate for the standard deviation $\sigma = 0.0031$.

All computed reconstructions are Maximum A Posteriori (MAP) estimates, utilizing the noise model (9) and prior model

$$X \sim \mathcal{N}(0, \zeta^2 I). \quad (10)$$

For the experiments, the prior standard deviation was set to $\zeta = 2.5 \cdot 10^{-4}$, and the feasibility of the selection was verified by visual assessment of the full domain local tomography reconstruction using the model $b = Ax$. The MAP estimate using the full domain model is shown in Figure 1. The spotlight part of the full domain model solution, shown on the right, is the restriction of the solution to the ROI, and it serves as the ground truth for the estimates computed based on the spotlight model A_1x_1 . We denote the spotlight part of the MAP estimate with the model Ax , or ground truth, as x_1^* . To assess the performance of the spotlight inversion, we define the relative error of any reconstruction x_1 by the formula

$$d(x_1, x_1^*) = \frac{\|x_1 - x_1^*\|}{\|x_1^*\|} \quad (11)$$

To test the projection model, we computed SVD of A_2 and computed the clutter-to-noise ratio curve R_r in equation (6), which is shown in Figure 2. The clutter-to-noise ratio criterion (7) yielded an optimal truncation parameter $r = 587$ for the approximate projection $P_r^\perp = I - U_r U_r^\top$.

Figure 3 shows the MAP estimates using the different models. For convenience, top left shows the reference image x_1^* explained above. Top right shows the MAP estimate using the naïve reduced model

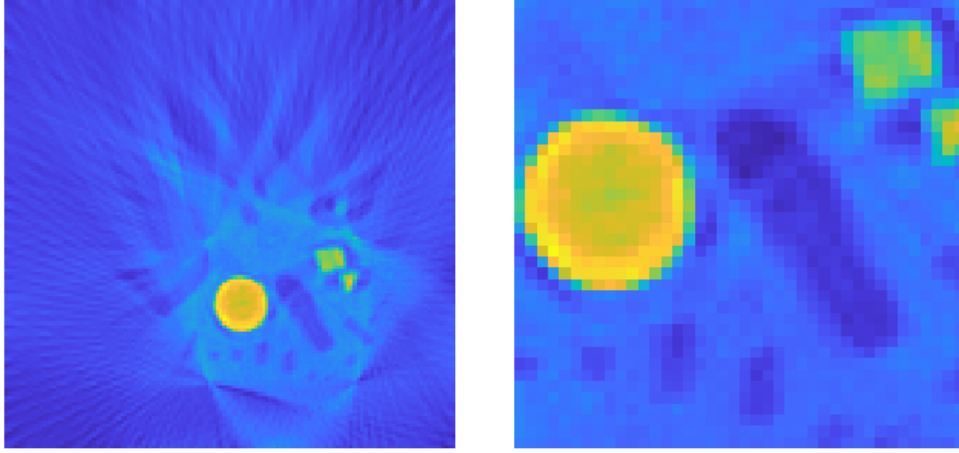


Figure 1: Left: The MAP estimate from local tomography data using the full domain model $b = Ax$. Right: Spotlight part from the MAP estimate on the left. We denote the spotlight part as x_1^* and use it as ground truth reference for the estimates computed using the spotlight model A_1x_1 .

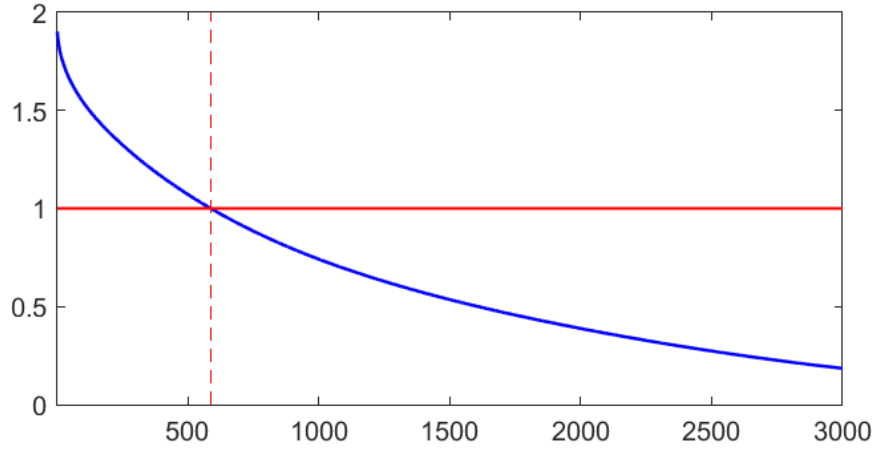


Figure 2: Clutter-to-noise ratio R_r for the local tomography experiment. Horizontal axis is the number r of svd vectors (i.e., number of columns in U_r). The point where $R_r = 1$ is at $r = 587$, denoted by the red dashed line.

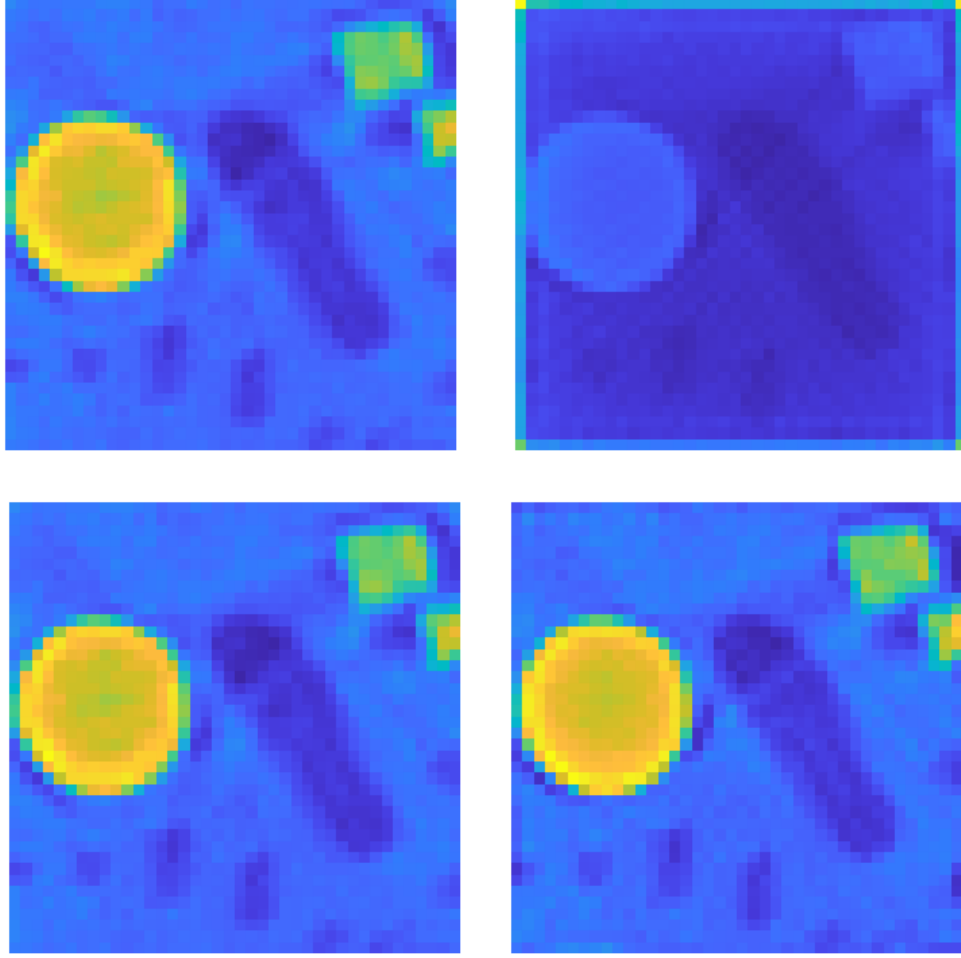


Figure 3: Top left: Reference solution x_1^* (detail from the MAP estimate with the full model Ax). Top right: MAP estimate using the naïve model $b = A_1 x_1$ that ignores the clutter (relative error: $d(x_1, x_1^*) = 1.51$). Bottom left: MAP estimate from marginal density $\pi_{X_1|B}(x_1 | b)$ (relative error: $d(x_1, x_1^*) \approx 10^{-15}$). Bottom right: MAP estimate using the projected spotlight model $P_r^\perp b = P_r^\perp A_1 x_1$ with $r = 587$ (relative error: $d(x_1, x_1^*) = 0.0596$).

$b = A_1 x_1$, assuming that contribution of the density distribution outside the spotlight domain is negligible, i.e., approximating $A_2 x_2 \approx 0$. As can be seen, the estimate exhibits large image artifacts, especially near the boundaries of the spotlight domain, and it lacks in dynamical range, with the relative error compared to the reference x_1^* (top left) around 150%. The bottom left shows the MAP estimate from the marginal density $\pi_{X_1|B}(x_1 | b)$, the mean μ_1 of the marginal density of Theorem 1.1, which is, as expected, close to the reference x_1^* from the MAP estimate with the full local tomography model Ax . The bottom right shows the MAP estimate with the projected spotlight model $P_r^\perp b = P_r^\perp A_1 x_1$ with $r = 587$, the truncation parameter value obtained by the cSNR analysis. The estimate is qualitatively very similar to the reference, with the relative error being around 6%.

To study the effect of the SVD truncation parameter r , we computed MAP estimates for a range of number of SVD components (i.e. number of columns in U_r) included in the approximate projector. The estimation errors $d(x_1, x_1^*)$ with respect to truncation parameter r are shown in Figure 4. We observe that the

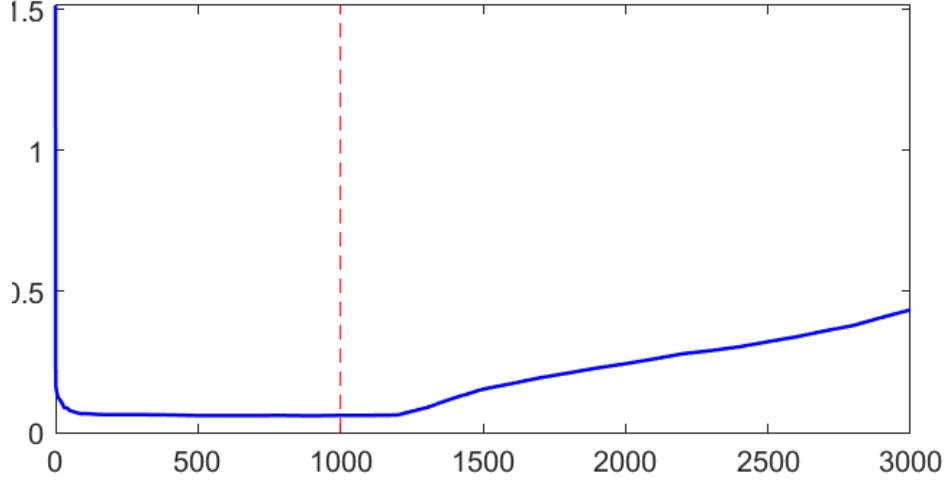


Figure 4: Estimate error $d(x_1, x_{*,1})$ with respect the truncation radius r in the projection model. The minimum error is at $r = 1000$ with $d(x_1, x_{*,1}) = 0.0595$

estimation error demonstrates a typical semi-convergence behavior, which can be understood through an SNR analysis: For small r , the clutter term dominates, while for high r , the projector P_r^\perp starts to erode the information contents of the informative term $P_r^\perp A_1 x_1$, leading eventually to poor reconstruction. The smallest estimation error occurs at $r = 1000$ with $d(x_1, x_1^*) = 0.0595$, suggesting that the selection of the truncation parameter by using the clutter signal-to-noise ratio led to a highly feasible selection, as the difference in the relative error with $r = 587$ was only 0.01% compared to the minimum at $r = 1000$. We observe from Figure 4 that the estimation error curve plateaus fast with respect to the number of SVD components, suggesting that already a relatively low number of singular vectors are enough for effective projection. For comparison, the right image in Figure 5 shows the MAP estimate with $r = 100$, with the relative error being only slightly larger than with the estimate with the selection of r based on the clutter signal-to-noise ratio (bottom right in Figure 3) or in the estimate with the smallest error compared to reference x_1^* with $r = 1000$.

5 Conclusions and outlook

This article proposes a purely linear algebraic approach for reducing a linear forward model with clutter, a linear contribution from a nuisance parameter, which, in spite of its limitations, is a commonly encountered type of clutter in practical inverse problems. The results with the computed example indicate that this approach allows computationally efficient treatment of clutter. In high resolution problems in three and four dimensions where time dependency enters, the use of full model or marginalization can be computationally expensive, while the proposed spotlight projection model allows computationally efficient treatment of clutter. In practice, and in light of some preliminary tests, we expect that one would need only few hundreds of left singular vectors of A_2 to reduce significantly the clutter, whereby the methods of randomized linear algebra will be of utmost utility.

The proposed projection method has direct connections to earlier works on nuisance parameter estimation.

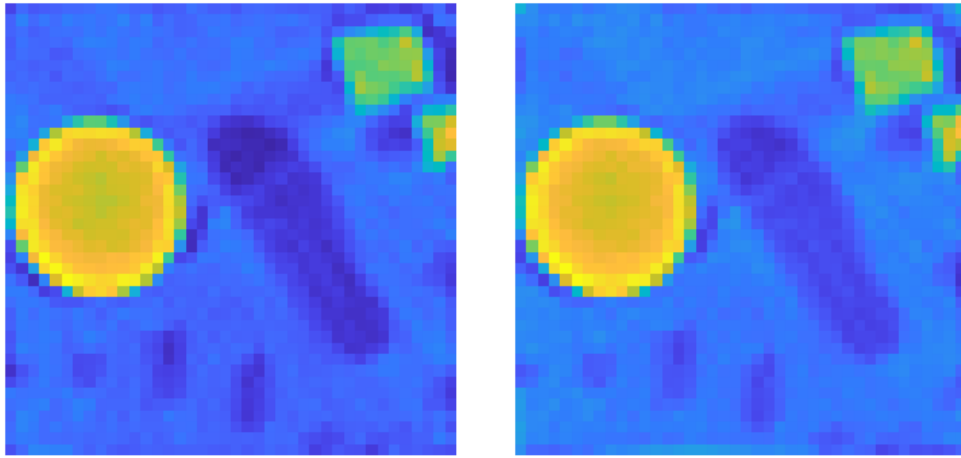


Figure 5: Left: MAP estimate with the projected model $P_r^\perp b = P_r^\perp A_1 x_1$ with $r = 1000$ corresponding to the minimum point in Figure 4 ($d(x_1, x_{*,1}) = 0.0595$). Right: MAP estimate with $r = 100$ (relative error: $d(x_1, x_{*,1}) = 0.0667$).

In fact, the formula (3) is a version of the likelihood factorization methods [2], taking advantage of the known fact that independency and orthogonality in the Gaussian framework coincide. This connection may provide new ideas of developing the more general nuisance parameter suppression methods towards an algorithmic direction.

The method has extensions to non-linear inverse problems, e.g., via applying spotlight inversion to equations obtained via sequential linearizations. Such an approach is particularly compelling if the range of the derivative with respect to the nuisance parameters is independent of the point at which it is evaluated; in fact, this study was inspired by such sensitivity analysis in [8] on electrical impedance tomography.

Acknowledgements

The work of DC was partly supported by the National Science Foundation (NSF) Division of Mathematical Sciences (DMS) grants 1951446 and 2513481, the Simons Foundation International (SFI) Mathematics & Physical Sciences (MPS) Simons Fellows in Mathematics (SFM) grant 00011595 and the SFI Travel Support for Mathematicians (TSM) grant 00007812. The work of ES was partly supported by the NSF grants DMS 2204618 and DMS 2513481. The work of NH and VK was supported by Research Council of Finland (RCF) Flagship of Advanced Mathematics for Sensing, Imaging and Modeling grant (nos. 358944 and 359181), the RCF Centre of Excellence in Inverse Modelling and Imaging grant (nos. 353084 and 353081) and RCF grants (nos. 359433 and 359434).

References

- [1] A. Y. ARAVKIN AND T. VAN LEEUWEN, *Estimating nuisance parameters in inverse problems*, Inverse Problems, 28 (2012), p. 115016.

- [2] D. BASU, *On the elimination of nuisance parameters*, in Selected Works of Debabrata Basu, Springer, 2010, pp. 279–290.
- [3] J. O. BERGER, B. LISEO, AND R. L. WOLPERT, *Integrated likelihood methods for eliminating nuisance parameters*, Statistical science, 14 (1999), pp. 1–28.
- [4] T. A. BUBBA, A. HAUPTMANN, S. HUOTARI, J. RIMPELÄINEN, AND S. SILTANEN, *Tomographic X-ray data of a lotus root filled with attenuating objects*, Sept. 2016.
- [5] D. CALVETTI AND E. SOMERSALO, *Bayesian scientific computing*, (2023).
- [6] A. DOUCET, S. J. GODSILL, AND C. P. ROBERT, *Marginal maximum a posteriori estimation using Markov chain Monte Carlo*, Statistics and Computing, 12 (2002), pp. 77–84.
- [7] N. HALKO, P.-G. MARTINSSON, AND J. A. TROPP, *Finding structure with randomness: Probabilistic algorithms for constructing approximate matrix decompositions*, SIAM review, 53 (2011), pp. 217–288.
- [8] A. JÄÄSKELÄINEN, J. TOIVANEN, A. HÄNNINEN, V. KOLEHMAINEN, AND N. HYVÖNEN, *Projection-based preprocessing for electrical impedance tomography to reduce the effect of electrode contacts*, arXiv preprint arXiv:2412.15009, (2024).
- [9] J. KAIPIO AND E. SOMERSALO, *Statistical inverse problems: discretization, model reduction and inverse crimes*, Journal of computational and applied mathematics, 198 (2007), pp. 493–504.
- [10] V. KOLEHMAINEN, T. TARVAINEN, S. R. ARRIDGE, AND J. P. KAIPIO, *Marginalization of uninteresting distributed parameters in inverse problems-application to diffuse optical tomography*, International Journal for Uncertainty Quantification, 1 (2011).
- [11] J. V. LINNIK, *Statistical problems with nuisance parameters*, vol. 20, American Mathematical Soc., 2008.
- [12] P.-G. MARTINSSON AND J. A. TROPP, *Randomized numerical linear algebra: Foundations and algorithms*, Acta Numerica, 29 (2020), pp. 403–572.
- [13] A. G. RAMM AND A. I. KATSEVICH, *The Radon transform and local tomography*, CRC press, 2020.
- [14] J. A. TROPP AND R. J. WEBBER, *Randomized algorithms for low-rank matrix approximation: Design, analysis, and applications*, arXiv preprint arXiv:2306.12418, (2023).